

Fabrication and Characteristics of Free Standing Shaped Pupil Masks for TPF-Coronagraph

Kunjithapatham Balasubramanian^{*1}, Pierre M. Echternach¹, Matthew R. Dickie¹, Richard E. Muller¹, Victor E. White¹, Daniel J. Hoppe¹, Stuart B. Shaklan¹, Ruslan Belikov², N. Jeremy Kasdin², Robert J. Vanderbei², Daniel Ceperley³, Andrew R. Neureuther³

Affiliation: ¹Jet Propulsion Laboratory, California Institute of Technology, Pasadena, CA, USA 91109, ²Princeton University, Princeton, NJ, USA 08544, ³University of California, Berkeley, CA, USA 94720.

ABSTRACT

Direct imaging and characterization of exo-solar terrestrial planets require coronagraphic instruments capable of suppressing star light to 10^{-10} . Pupil shaping masks have been proposed and designed¹ at Princeton University to accomplish such a goal. Based on Princeton designs, free standing (without a substrate) silicon masks have been fabricated with lithographic and deep etching techniques. In this paper, we discuss the fabrication of such masks and present their physical and optical characteristics in relevance to their performance over the visible to near IR bandwidth.

Keywords: Terrestrial Planet Finder, Coronagraph, shaped pupil mask, DRIE

1. INTRODUCTION

Shaped pupil coronagraphs have been proposed and studied for exo solar planet finding coronagraph architectures. Vanderbei *et al*^{2,3} reported several designs of pupil shaping masks aimed at achieving star light suppression to 10^{-10} level required for imaging terrestrial planets in the visible spectrum. Fabrication and testing of shaped pupil masks⁴ is currently under investigation at Princeton University and JPL. Recently, free standing masks with silicon were fabricated at JPL and tested at Princeton University and at JPL. In this paper, we discuss the fabrication and characteristics of these masks with initial results and challenges; details of the testing and contrasts obtained with a laser as well as a broadband source can be found in another paper of Belikov *et al*⁵.

2. DESIGN OF SHAPED PUPIL MASKS

Figure 1 shows the two shaped pupils that are the subject of this paper. Many practical constraints and trade-offs have guided the selection of these particular mask designs. The first choice made was to manufacture a free-standing Si mask with etched holes instead of a mask on a transparent glass substrate. This was because masks on a substrate glass suffer from multiple reflections leading to ghost images besides possible slight aberrations and sensitivity to polarization and dispersion. While in typical optical systems, high quality glasses and anti reflection coatings render these effects all but negligible, the high contrast required for Earth-like planet detection may be degraded by even the smallest of defects in the highest quality glass.

The second choice to be made was the actual shape of the mask. Attention to practical considerations for free-standing masks has guided the selection of the design in this case as well. The options initially included barcode, cross-barcode, concentric ring, spiderweb, starshape, and ripple designs². Except for the ripple

* Corresponding author email: kbala@jpl.nasa.gov; phone: 1-818-393-0258

designs, all others have either unsupported or not structurally stable elements, or slits/apertures that are too small (much smaller than the minimal thickness of the mask). The ideal design that would support ease of manufacturing and ensure structural integrity would be a mask with minimum number of openings, and free of hanging structures and thin long ribbons. The ripple designs generally satisfy these requirements, and we selected two of them, shown in Figure 1.

Ripple 1, intended for an elliptical pupil, has 6 slits of varying shapes and slit widths with an opaque bar region in the middle. A pin hole (not visible in the figure) is also incorporated in the center of the mask for wavefront diagnostics. Ripple 3, intended for a circular pupil, has 7 slits of varying shapes with no central obscuration. These masks for initial experiments were designed to perform to contrast levels of about 10^{-8} at an inner working angle of $4\lambda/D$.

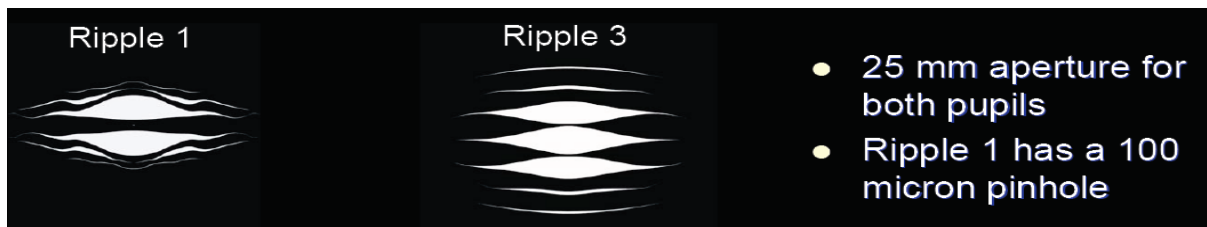


Figure 1. Typical Shaped Pupil Masks designed by Princeton University Fabricated at JPL for tests at JPL’s High Contrast Imaging Testbed (HCIT)

Slit cross-section:

The manufactured masks differ from the designed masks due to finite mask thickness and finite conductivity. Quantitative analysis of the differences between thin-mask scalar diffraction theory (used to design the mask) and thick-mask vector diffraction simulations uncovered a number of physical sources of light scattering (stray-light, Figure 2) that are not modeled by scalar theory and necessitate adjustments to the manufacturing process. The largest source of stray-light comes from diffraction confinement by thick-mask sidewalls, which effectively bias a mask opening by up to 3 wavelengths per edge; however, this electromagnetic bias can be reduced by an order of magnitude by undercutting the sidewalls 20 degrees. Dependencies on

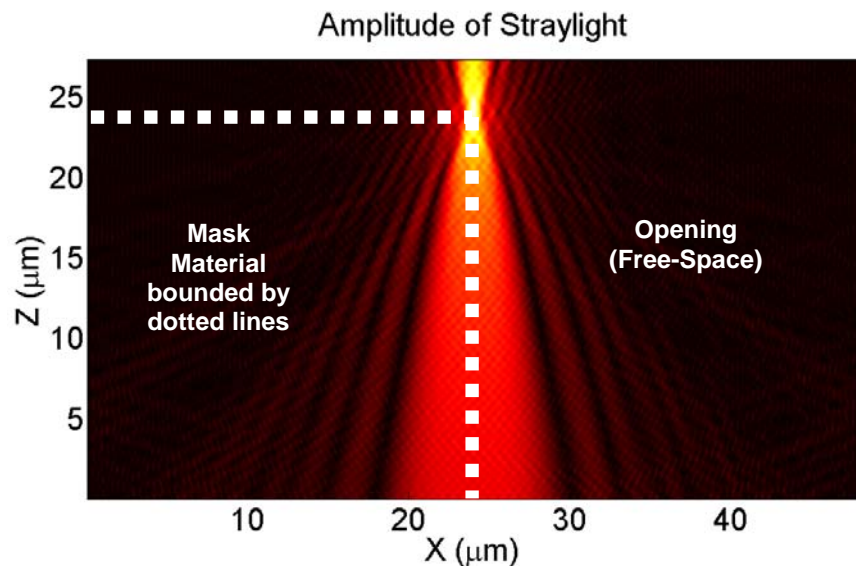


Figure 2: Image of stray-light along the left sidewall of an opening in a pupil mask. Adding this light into the thin-mask scalar model adjusts the diffraction pattern to match the results from thick-mask vector simulation. This particular stray-light image was taken from a simulation of a 48micron wide opening in a 50micron thick Silicon mask with vertical sidewalls and a 200nm Chrome top coat at a wavelength of 630nm.

polarization and wavelength create additional stray-light; however, these effects bias the mask opening by only a quarter wavelength per edge. Narrow openings (less than 20 wavelengths wide) see much stronger effects with up to 7 wavelengths of bias per edge (on a 100 μm thick mask) which greatly changes the performance of the opening. Details of these studies can be found in a paper by Ceperley et al.⁶. Manufacturing roughness, in the form of horizontal corrugations and vertical erosions, create additional stray-light by narrowing openings and introducing cross-polarization on sharp features.

Guided by such vector diffraction models of thick masks, and for ease of fabrication in our initial attempts, we incorporated a step instead of the desired 20 degree undercut of sidewalls. Figure 3 shows nominal cross section of the wall and step around the apertures with such an approach.

The thinned region of the mask demanded an overcoat of aluminum to prevent leakage of light in the near IR region due to the transparency of silicon. We employed a float zone material double side polished <100> plane nominally 400 microns thick silicon wafer. The N type phosphorous doped silicon with a refractive index of 3.693 and extinction coefficient of 0.007 at 785nm shows an optical density of about 3 for a thickness of 50 microns. Adding a layer of Al helps to increase the optical density to >12 in the near IR wavelengths.

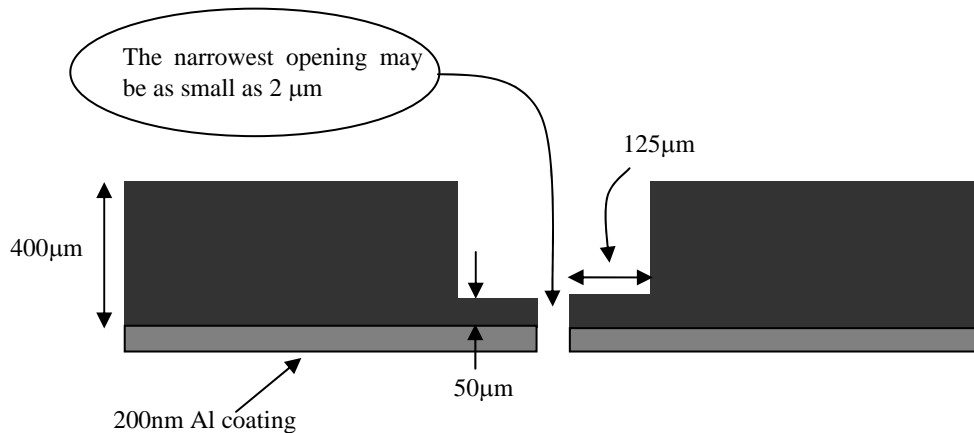


Figure 3. Mask slit / aperture design showing recessed step around slits / apertures

3. FABRICATION OF DEEP ETCHED SILICON MASKS

Shaped pupil masks without a supporting substrate require an appropriate material and fabrication technique to form precisely shaped slits and apertures with micron scale accuracies. Deep reactive ion etching (DRIE) techniques have been developed for micromachining of deep trenches in silicon. The process known as “Bosch” process⁷ initially developed by Robert Bosch GmbH has been adopted and developed to fabricate MEMS devices for various applications⁸. Hence, silicon and the DRIE process show promise for accurate fabrication of shaped pupil masks for TPF coronagraph as demonstrated by our experiments.

The equipment and technique: At JPL, we employ a Surface Technology Systems (STS) Inductively Coupled Plasma (ICP) etching system for fabricating deep trenches in silicon. The STS system utilizes inductively coupled time multiplexed plasmas of SF_6 and C_4F_8 gases in order to anisotropically etch silicon. The C_4F_8 and SF_6 plasmas sequentially passivate and etch the silicon until a desired depth is reached. This technique can lead to very high aspect ratios (up to 30:1), profile control (up to 90 degrees) and high etch rates (up to 6 microns/min). Details and variations of the basic process can be found in various references^{9,10}.

Extending this technique to etch apertures through 400 microns thick silicon wafers presented challenges and required a few trials and process optimization.

The slits and apertures as per the cross section with recessed steps shown in figure 3 were generated by two etching cycles, one from the front side and the other from the back side. Two photo masks for the two sides were first fabricated by ebeam lithography. The etch depths for the two sides were controlled so as to punch the wafer through leaving the designed step height.

4. MASK CHARACTERISTICS OPTICAL AND SEM INSPECTIONS

Several samples of various shapes and sizes of masks for elliptical and circular pupils were fabricated on nominally 400 microns thick silicon wafers. The smallest size that we attempted to fabricate was a 10mm elliptical mask intended for working with a 10mm deformable mirror (DM) enabled coronagraph test bed at Princeton. Larger masks of the Ripple 1 and Ripple 3 shapes were fabricated for tests at Princeton without a DM and also at JPL's High Contrast Imaging Testbed (HCIT) which employs a 32x32mm DM. Some of these masks were overcoated with aluminum to determine performance differences with uncoated ones, at short and long wavelengths.

The masks were inspected for quality and defects with optical and electron microscopes. A typical 25X magnified image of a section of the mask showing two of the curved slits in Ripple 1 type mask (not the actual mask used in the HCIT) is shown in figure 4. The gray regions surrounding the apertures (seen as dark area in the figure) are the recessed steps as per figure 2. The crisply etched steps along the slit edges are seen clearly in figure 5. However, it was observed that the actual widths of these recessed steps were slightly different from expected values. Similarly, the thickness of the recessed steps was also larger than the design in this particular sample. However, these differences did not seriously affect the mask performance.

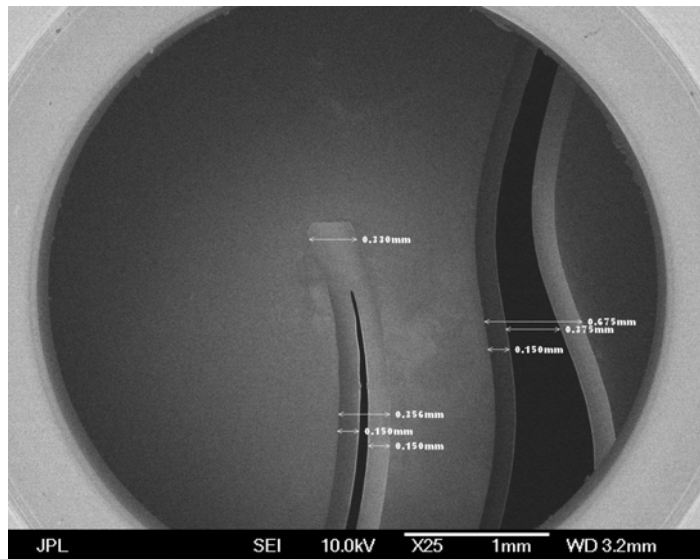


Figure 4. Typical shape and image of apertures of an actual mask fabricated by DRIE technique

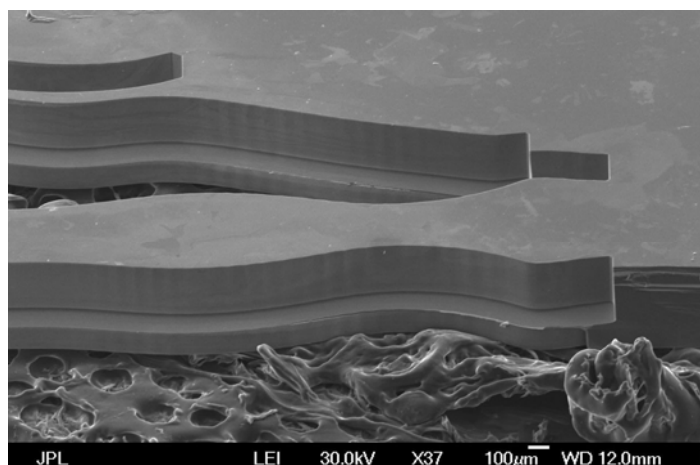


Figure 5. A mask slit seen under SEM showing recessed steps surrounding the slits

A few minor defects due to incomplete etching were also seen in a few spots especially at the smallest slit dimensions. Another significant observation is the pronounced roughness at the corners of wall edges. Figure 6 shows the nature of the aperture walls as a consequence of the passivation and etching process sequence to get through the entire etch depth. Higher magnifications reveal finer features of the wall shown in figures 6 and 9.

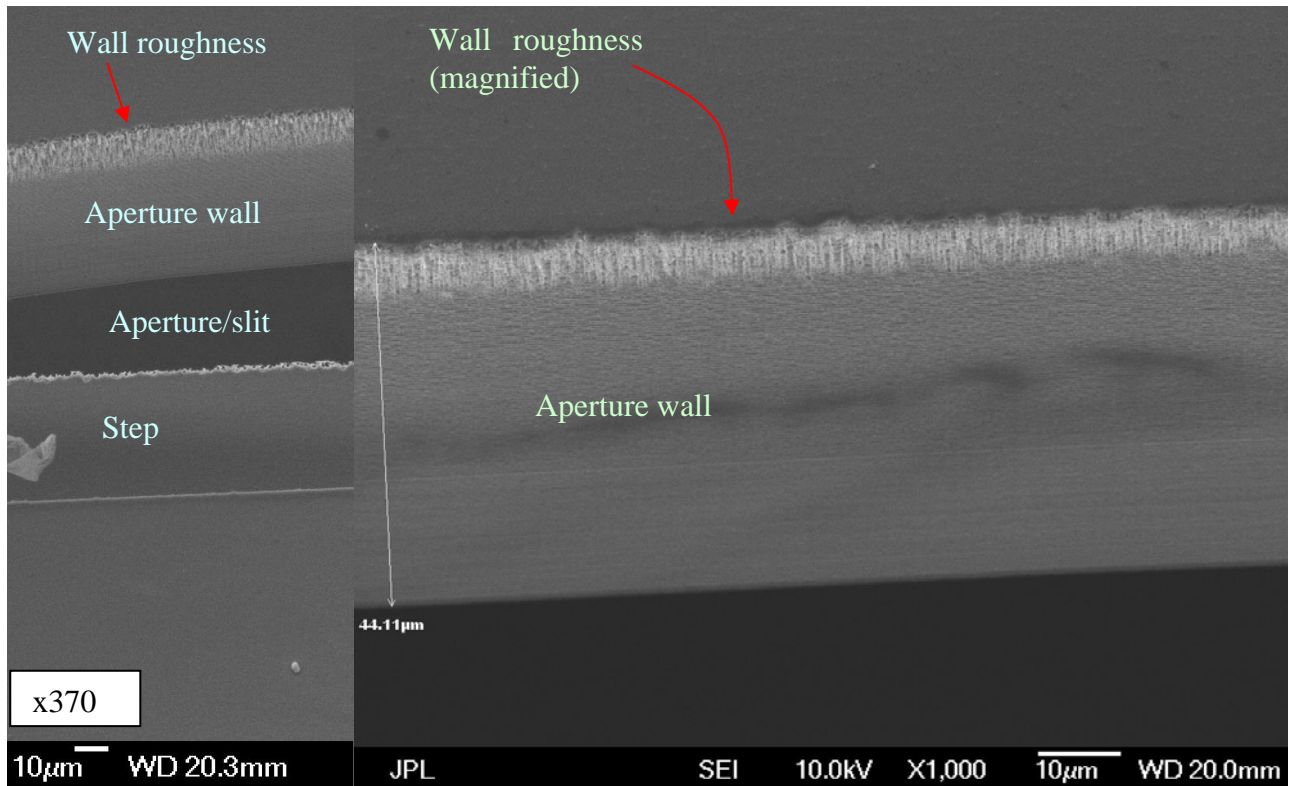


Figure 6. Left: Aperture and wall seen at 20 deg tilt angle with 370x magnification in an SEM. Right: Aperture wall seen at 20 deg tilt with 1000x magnification; see figure 9 for 5000x magnified image of the same sample showing vertical and horizontal striations in the wall edge.

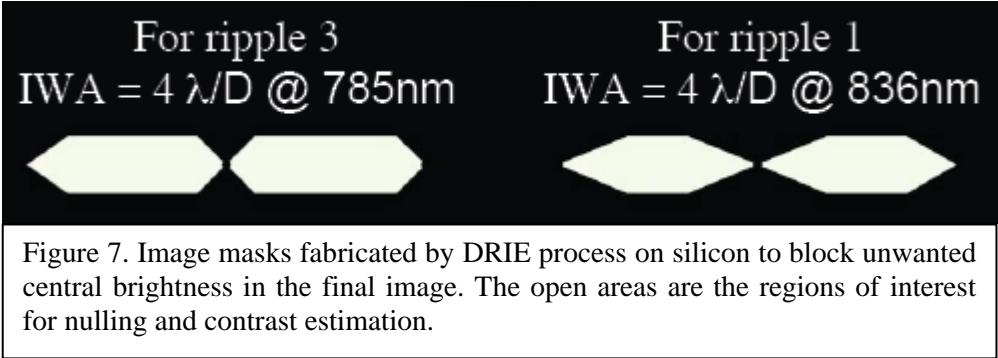


Figure 7. Image masks fabricated by DRIE process on silicon to block unwanted central brightness in the final image. The open areas are the regions of interest for nulling and contrast estimation.

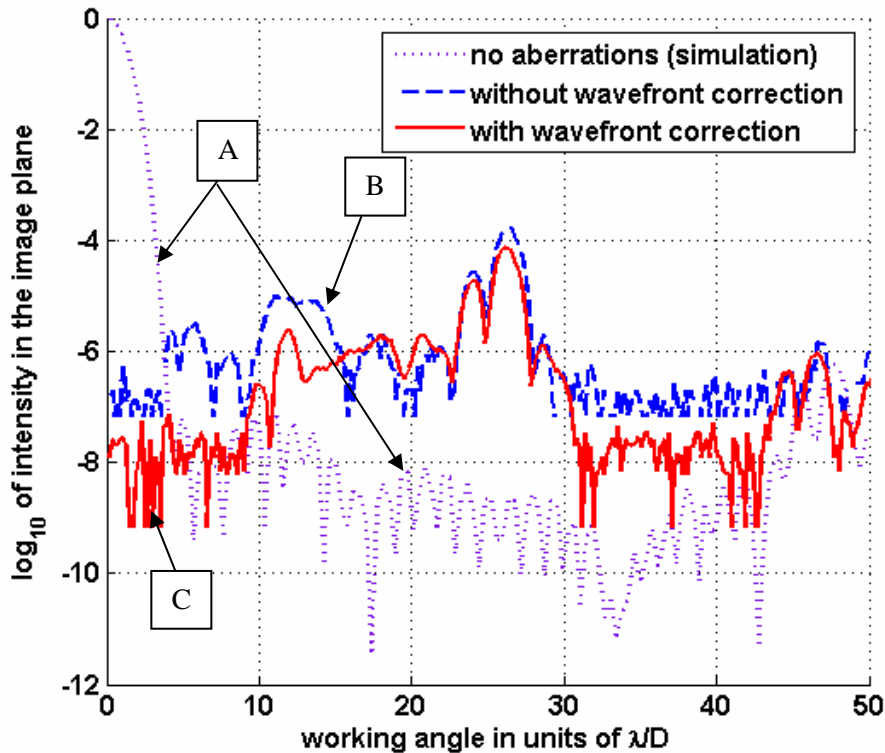
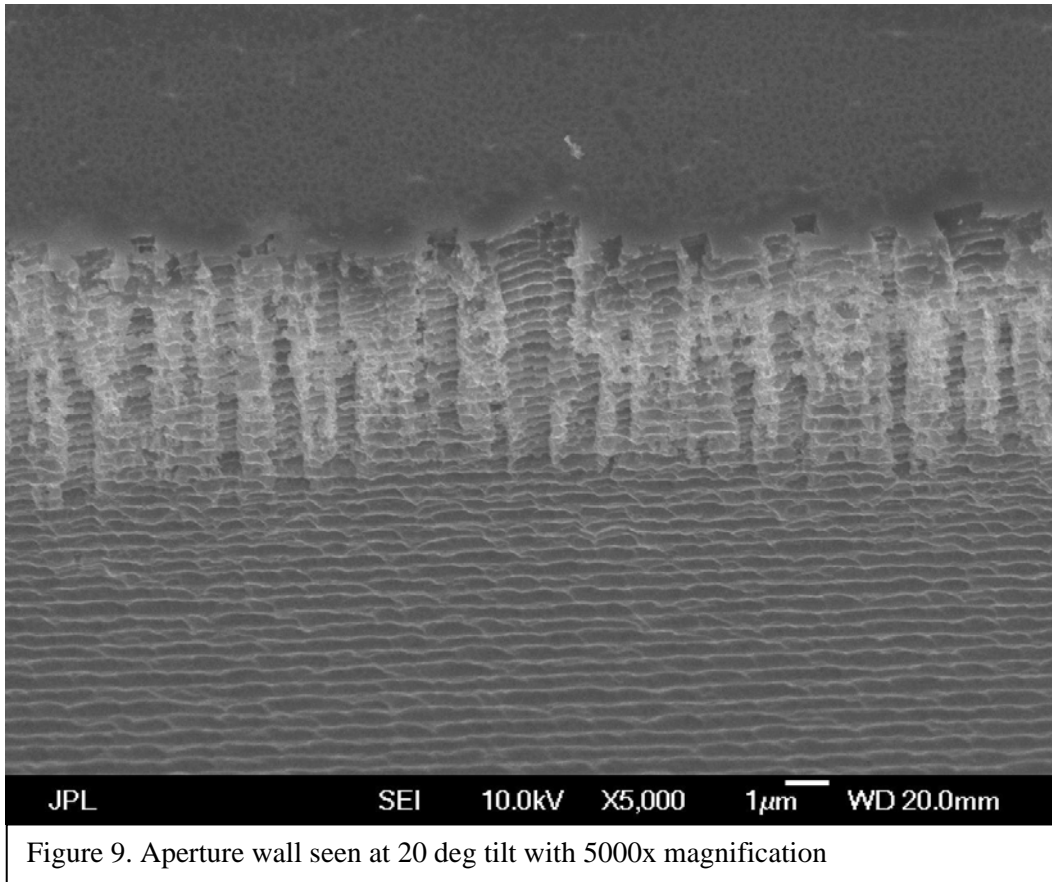


Figure 8. Simulated (A) and measured (B and C) image intensity plots when ripple 3 mask and corresponding image mask are employed in the HCIT

5. INITIAL RESULTS WITH SHAPED PUPIL MASKS

Both Ripple 1 and Ripple 3 have been tested on JPL's High Contrast Imaging Testbed (HCIT), which is described in detail in Belikov *et al*⁵. In short, the HCIT essentially simulates a star, lets it propagate through one of several coronagraph configurations, and takes a CCD image of the suppressed star and any diffracted light around it. Figure 8 shows 3 cross-sections through the CCD images when using Ripple 3 under monochromatic 785nm light. The simulated plot (curve A) shows the "ideal" point spread function, i.e. how a star would appear after going through the shaped pupil coronagraph with ideal optics. Note that the main lobe of the star is not suppressed in the simulation in order to show its shape. In theory, it's not necessary to suppress the main lobe, but in practice it will overwhelm the CCD, so it is blocked by an image plane mask (as shown in figure 7), located downstream from the shaped pupil. These masks were also fabricated on silicon by the same DRIE process. The "ideal" plot (curve A) in figure 8 shows that Ripple 3 was designed to achieve better than 10^{-7} contrast for working angles $>4\lambda/D$.

The blue plot (curve B) shows the measured image cross section intensity, showing a somewhat degraded contrast due to the slight wavefront imperfections of the HCIT optics that are present without wavefront correction. HCIT employs a high quality Xinetics deformable mirror to correct for these aberrations, and the contrast is seen to improve by more than a factor of 100 with these corrections as seen in curve C. This



proves that the manufacturing process is successful at producing a shaped pupil mask that performs to designed specifications, when used with a wavefront control system.

6. CHALLENGES

The promising results of these preliminary experiments with free standing shaped pupil masks fabricated by DRIE process exposes some of the challenges in design and fabrication of these masks. Thicker silicon wafers present etching challenges. Radial nonuniformity of etch rates leave inadequate etch depths at the edges relative to the central region. Secondly, the etch rate differences between wider slits and narrow slits result in inaccurate slit widths. Further, the nature of the DRIE process which involves repeated etching and passivation steps through the depth of etch results in typical wall roughness in the form of striations and curtain-like features as seen in figures 6 and 9 under high magnification. Such process dependent features¹¹ have also been studied by others and reported in the literature^{12, 13} with ideas to diminish the sidewall roughness. While such micron and sub-micron scale sidewall features may not present serious problems for other applications, diffraction and scattering through the apertures surrounded by these rough walls may limit the ultimately achievable contrast for TPF coronagraph. The above fabrication challenges and the requirements on mask stability and integrity will be addressed in our next experiments with further improvements in the design and fabrication of these masks. Process parameter modifications coupled with the use of silicon-on-insulator (SOI) type wafers are expected to yield better results.

7. CONCLUSIONS AND FUTURE STEPS

Our first set of experiments with the fabrication and testing of silicon based free standing shaped pupil masks have yielded coronagraph contrasts of about 4×10^{-8} with monochromatic (785nm laser) and 5×10^{-8} with a broadband (10% BW around 800nm) source. Details of the measurements and nulling techniques can be found in Belikov *et al* paper⁵ in this volume of SPIE proceedings. The DRIE technique investigated here promises manufacturability of pupil masks with adequate accuracy, particularly with technology developments through further experiments. Our next steps aim at process optimization to obtain uniform etch rates over wide areas and different aspect ratios, elimination of aperture wall roughness, use of SOI wafers, and optimization of designs that may avoid very narrow slits that are prone to fabrication errors.

8. ACKNOWLEDGEMENTS

This work was performed at the Jet Propulsion Laboratory, California Institute of Technology, in collaboration with Princeton University and the University of California Berkeley, under a contract with the National Aeronautics and Space Administration. Reference herein to any specific commercial product, process or service by trade name, trademark, manufacturer, or otherwise, does not constitute or imply its endorsement by the United States Government or the Jet Propulsion Laboratory, California Institute of Technology.

9. REFERENCES

-
- 1) N. J. Kasdin, R. J. Vanderbei, D. N. Spergel, and M. G. Littman, "Extrasolar planet finding via optimal apodized-pupil and shaped-pupil coronagraphs," *The Astrophysical Journal*, Vol. **582**, pp. 1147–1161, (2003).
 - 2) R. J. Vanderbei, Spergel D. N., Kasdin N. J., and Kuchner M., "New Pupil Masks for High-Contrast Imaging" *in Techniques and Instrumentation for Detection of Exoplanets*, Ed. Daniel R. Coulter, *Proc. of SPIE*, **5170**, pp.49-56, (2003).
 - 3) N. Jeremy Kasdin, Robert J. Vanderbei, Michael G. Littman, Michael Carr and David N. Spergel, "The Shaped Pupil Coronagraph for Planet Finding Coronagraphy: Optimization, Sensitivity, and Laboratory Testing", *Proc SPIE* vol. **5487**, pp 1312-1321, (2004).
 - 4) N. Jeremy Kasdin, Ruslan Belikov, James Beall, Robert J. Vanderbei, Michael G. Littman, Michael Carr, and Amir Give'on, "Shaped Pupil Coronagraphs for Planet Finding: Optimization, Manufacturing, and Experimental Results", *in Techniques and Instrumentation for Detection of Exoplanets II*, edited by Daniel R. Coulter, *Proceedings of SPIE* Vol. **5905**, pp. 590950G1-G8, (2005)
 - 5) Ruslan Belikov, Amir Give'on, Michael Carr, John Trauger, Fang Shi, [Kunjithapatham Balasubramanian](#), Andreas Kuhnert, Jeremy Kasdin, "Towards 10^{-10} Contrast for Terrestrial Exoplanet Detection: Demonstration of Extreme Wavefront Correction in a Shaped-Pupil Coronagraph", in this conference proceedings, *Proc. SPIE* vol. **6265**-42, (2006)
 - 6) D. Ceperley, A. Neureuther, M. Miller, M. Lieber, and J. Kasdin, "Stray-Light Sources from Pupil Mask Edges and Mitigation Techniques for the TPF Coronagraph," in this conference proceedings, *Modeling, Systems Engineering, and Project Management for Astronomy II*, *Proc. SPIE* vol. **6271**-60, (2006).
 - 7) Method of anisotropically etching silicon – US Patent 5,501,893, Authors: Franz Laermer, and Andrea Schilp, assigned to Robert Bosch GmbH, Germany, March 26, (1996).

-
- 8) L.A. Donohue, J. Hopkins, R. Barnett, A. Newton, and A. Bark, "Developments in Si and SiO₂ Etching for MEMS based optical applications", *Micromachining Technology for Micro-Optics and Nano-Optics II*, edited by Eric G. Johnson, Gregory P. Nordin, Proc. SPIE vol. **5347**, pp. 44-53, (2004).
- 9) J.K. Bhardwaj., H. Ashraf., "Advanced Silicon Etching Using High Density Plasmas", in *Micromachining and Microfabrication Process Technology*, Proc. SPIE Vol. **2639**, pp.224-233, (1995).
- 10) J. Bhardwaj, H. Ashraf, and A. McQuarrie, "Dry Silicon Etching For MEMS", Presented at the The Symposium on Microstructures and Microfabricated Systems at the Annual Meeting of the Electrochemical Society, Montreal, Quebec, Canada, May 4-9, (1997).
- 11) Jae-Ho Min, Gyeo-Re Lee, Jin-Kwan Lee, and Sang Heup Moona, Chang-Koo Kim, "Angular dependence of etch rates in the etching of poly-Si and fluorocarbon polymer using SF₆, C₄F₈, and O₂ plasmas", *J. Vac. Sci. Technol. A* Vol.22, No.3, May-Jun 2004
- 12) M. Chabloz, Y. Sakai, T. Matsuura, and K. Tsutsumi, "Improvement of sidewall roughness in deep silicon etching", *Microsystems Technologies*, Vol. 6 (3), pp 86-89, (2000).
- 13) Chienliu Chang, Yeong-Feng Wang, Yoshiaki Kanamori, Ji-Jheng Shih, Yusuke Kawai, Chih-Kung Lee, Kuang-Chong Wu and Masayoshi Esashi, "Etching submicrometer trenches by using the Bosch process and its application to the fabrication of antireflection structures", *J. Micromech. Microeng.* Vol. 15, pp 580-585, (2005)